Journal of Renewable Energies

Revue des Energies Renouvelables

journal home page: https://revue.cder.dz/index.php/rer

Research paper

Design and testing of a parabolic solar concentrator with automatic tracking system

Youcef Mebarki [a], **Abdelhakim Belkaid** [b,*]

[a] *Laboratory LMER University A. Mira of Bejaia, Algeria.*

[b] *Laboratory LTII University A. Mira of Bejaia, Algeria.*

ARTICLE INFO

Article history:
Received April 3, 2024
Accepted April 25, 2024

Keywords:
Parabolic concentrator
Solar radiation
Absorber
Reflector
Heat-transfer fluid

ABSTRACT

The undertaken work revolves around an experimental investigation into harnessing solar energy and its conversion into thermal energy through the utilization of a parabolic concentrator. Ensuring optimal orientation concerning solar radiation is facilitated by an automatic tracking system. The prototype employed for testing primarily consists of a solar reflector, shaped as a parabola to efficiently reflect solar radiation, and an absorber comprising a coiled copper tube, designated as the focal point for concentrating the sun's rays. The attained results are significant, with temperatures surpassing 380°C recorded on the absorber's surface.

1. INTRODUCTION

In the quest for sustainable energy solutions, harnessing solar power has emerged as a pivotal avenue, offering abundant, clean, and renewable energy. Among the various solar technologies, parabolic solar concentrators stand out for their efficiency in concentrating sunlight onto a focal point, thus enabling the conversion of solar energy into usable thermal energy (Mohamed 2021). The effectiveness of such concentrators is further enhanced when coupled with automatic tracking systems, ensuring optimal alignment with the sun's trajectory throughout the day.

This research paper delves into the design and testing of a parabolic solar concentrator integrated with an automatic tracking system, aimed at maximizing solar energy capture and thermal output. The utilization of parabolic geometry facilitates the concentration of sunlight onto a focal point, where an absorber material efficiently converts it into thermal energy. The incorporation of an automatic tracking system ensures that the concentrator maintains alignment with the sun's position, optimizing energy capture and enhancing overall system performance.

[*] *Corresponding author, E-mail address: abdelhakim.belkaid@univ-bejaia.dz*
Tel :+ 213 796747339

ISSN: 1112-2242 / EISSN: 2716-8247

The design phase of this study involves meticulous consideration of various parameters, including the geometrical characteristics of the concentrator, the selection of materials for reflectors and absorbers, and the mechanisms for automatic tracking. Through comprehensive modeling and simulation, the optimal design parameters are identified to achieve maximum solar energy conversion efficiency.

Subsequently, experimental testing is conducted to validate the performance of the designed parabolic solar concentrator with an automatic tracking system. Real-world conditions are simulated to assess the system's ability to track the sun accurately and consistently, as well as its effectiveness in converting solar energy into thermal energy. Temperature measurements at the focal point provide crucial insights into the concentrator's thermal performance under varying solar conditions.

The outcomes of this research hold significant implications for the advancement of solar energy technologies, particularly in the realm of concentrating solar power (CSP) systems. By enhancing the efficiency and reliability of parabolic solar concentrators through automatic tracking, this study contributes to the ongoing efforts to harness solar energy more effectively and sustainably. Through a combination of theoretical analysis and practical experimentation, this paper aims to provide valuable insights into the design and optimization of solar concentrator systems for renewable energy generation.

Algeria is one of the sunniest countries in the world which led us to be interested in this discipline (Gamma 2008, Nadir 2012).

2. MECHANICAL MANUFACTURING

2.1 The reflector

We meticulously affixed small squares of mirrors onto a parabolic plate using thermal glue, ensuring a perfect fit to the curved interior surface. The mirrors were strategically selected for their exceptional 99.9% reflection rate, with their shiny sides meticulously positioned to face the sun, optimizing solar energy capture.

Table 1 Detailed Description of Reflector's Physical Attributes

Big diameter	d = 0.9 m
Little diameter	h = 0.08m
The opening angle	Ψ_p= 38.95°
Focal distance	f = 0.6328 m
Opening surface	A_a= 0.6361 m ^{2}
Mirrorless mass	m = 4.3kg

2.2 The Concentrator

This parameter quantifies the amount of energy focused at the collector, delineating between two distinct methods of solar concentration: geometric concentration, which pertains to surface area, and optical concentration, which concerns flux density.

2.2.1 Geometric concentration

Determined by the ratio between the surface area of the collector's aperture (Aa) and that of the receiver (Ar), geometric concentration directly influences temperature elevation. Higher geometric concentration yields greater temperature escalation within the system.

$$Cg = \frac{A_a}{A_r} \quad (1)$$

2.2.2 Geometric concentration

This ratio quantifies the relationship between the energy absorbed by the surface of the absorber and the energy incident upon the aperture of the parabolic structure (Kedwards 1979):

$$C_o = \frac{\mathrm{Ir}}{\mathrm{Ia}} \tag{2}$$

Where, Iris the energy received at the aperture of the receptor, and Iois the energy received at the aperture of the paraboloid.

The concentration ratio of the parabolic concentrator is denoted as (Kedwards 1979):

$$\mathrm{C} = 4.\frac{\sin^2\psi}{\Theta^2} \tag{3}$$

The maximum concentration Cmax = 46250 occurs at ψ = 90°.

2.2.3 The energy received when a paraboloid opens

Considering that the energy corresponds to the amount of light reflected across the entire surface of the parabola, it's imperative to account for a differential region that can be integrated over the entire surface. The differential surface, denoted as (Stine 2001), is defined as:

$$\mathrm{d}A_s = \mathrm{I}.\,\mathrm{ds} \tag{4}$$

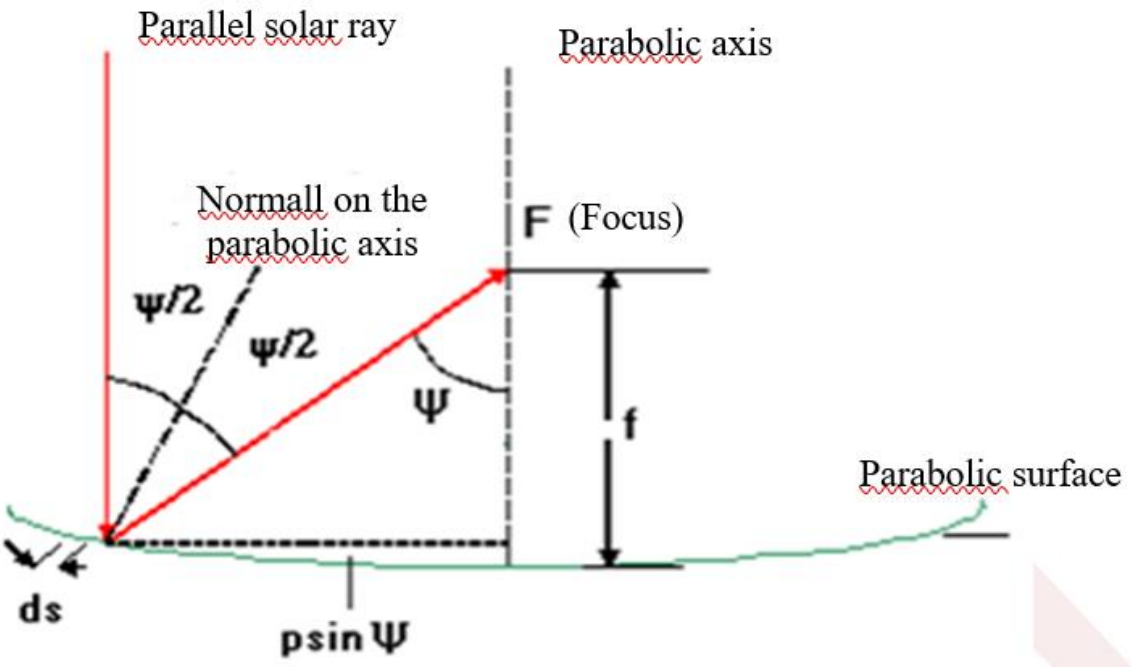

Fig. 1 Reflection of a parallel ray

Where:

ds represents the differential arc length of the parabola.

I denotes the length of a differential strip on the surface of a parabolic trough.

Since the angle $d\psi$ is small, we can approximate sin($d\psi$) as $d\psi$, thus simplifying the equation to:

$$\mathrm{ds} = \frac{\mathrm{p}\,\sin(\mathrm{d}\psi)}{\cos(\frac{\psi}{2})} = \frac{\mathrm{p}\,\mathrm{d}\psi}{\cos(\frac{\psi}{2})} \tag{5}$$

$$dA_s = \frac{I.p.d\psi}{\cos(\frac{\psi}{2})} \tag{6}$$

The radiant flux (dIa) reflected from this differential sector at the focal point is described by equation (7) as in (Stine 2001):

$$\mathrm{dI_a} = \mathrm{dA_s}.\mathrm{I_b}.\cos\left(\frac{\psi}{2}\right) = \mathrm{I}.\mathrm{p}.\mathrm{I_b}.\mathrm{d}\psi \tag{7}$$

Substituting the value of *p*, we obtain:

$$\mathrm{dI_a} = \frac{2.\mathrm{f}.\mathrm{I}.\mathrm{Ib}.\mathrm{d}\psi}{(1+\cos\psi)} \tag{8}$$

$$\mathrm{I} = \frac{4.\pi.\mathrm{f}.\sin\psi}{(1+\cos\psi)^2} \tag{9}$$

The energy received upon the aperture of a paraboloid is defined in reference (Kurzweg 1982) :

$$\mathrm{I_a} = \int \frac{8.\pi.\mathrm{Ib}.\mathrm{f}^2\sin\psi.\mathrm{d}\psi}{(1+\cos\psi)^2} \tag{10}$$

2.2.4 Solar power absorbed by the opening of the receiver

Upon reaching the aperture, this power experiences reductions due to losses, described by the following formula (Stine 2001):

$$\mathrm{Qa} = \mathrm{Ib}\,.\mathrm{Aa}\,.\alpha\,.\rho\,.\tau \tag{11}$$

$$\eta\mathrm{op} = \mathrm{Aa}\,.\alpha\,.\rho\,.\tau \tag{12}$$

Equation (11) is transformed into:

$$\mathrm{Qa} = \mathrm{Ib}\,.\eta\mathrm{op} \tag{13}$$

Where:

ηopis the Optical efficiency of the concentrator, Ibis the Energy received at the concentrator aperture, τ is the Receiver transmission coefficient, α is the Absorption coefficient of the receiver, and ρ is the Reflectance coefficient of the parabola.

2.3 The Absorber

The absorber requires high thermal conductivity and a high melting or degradation point, leading us to select copper as the material for the absorbing device (with a thermal conductivity of 386 W/m·K and a melting point of 1083 °C) (Mebarki 2020). Constructed from a copper coil housed within a chimney pipe tube, insulated with glass wool for effective insulation, we also inserted aluminum foil pieces between the absorber and the inner wall of the tube to leverage cumulative temperature effects. The copper coil, originally 6mm in diameter and 1m in length, was modeled into a coil measuring 60 mm in diameter and 15 cm in length. This configuration was then placed within an 80mm diameter and 20 cm long chimney pipe, enclosed within another tube of the same material but 110 mm in diameter and 20 cm in length. The geometric concentration of this model is:

$$\mathrm{Cg} = \frac{\mathrm{Aa}}{\mathrm{Ar}} = \frac{0.6361}{0.00282} = 225.008 \tag{14}$$

Fig. 2 Real photo of the absorber

Table 2 Physical Attributes of the absorber

Coil diameter	d_2 = 0.06 m
Coil length	l_2 = 0.15 m
Capture surface	A_r = 0.002827 m^2
Mass of empty absorber	M_a = 0.5 Kg

2.3 Mechanism of tracking

The vertical rotation system is facilitated by an electric motor outfitted with a drive chain. We've incorporated additional support to enhance stability and fortify against wind-induced swaying. The system components were meticulously modeled using SolidWorks, a leading mechanical design and manufacturing software. Each element was assembled with meticulous attention to the specified constraints, ensuring the desired mechanism was achieved.

Fig. 3 Concentratorimage

Fig. 4 The prototype produced using SOLIDWORKS

3. THERMAL POWER LOSSES

Once solar energy reaches the opening surface of the receiver, its temperature exceeds the ambient temperature. This variance triggers heat dissipation, characterized by convection, radiation, and conduction. The power associated with these thermal losses can be quantified by the following expression (Bonned 2003):

$$Qp = Qp.cv + Qp.r + Qp.cd \quad (15)$$

Where

Qp: Thermal Loss Power

Qp.cv: Convection Losses

Qp.r: Radiation Losses

Qp.cd: Conduction Losses

3.1 Convection Losses

Convection loss occurs as heat dissipates to the surrounding air upon contact with the body's surface. The rate of heat transfer to cold air is influenced by the air's velocity and direction at the site. These losses are directly proportional to the receiver's surface area and the temperature differential between the absorber's surface and the ambient air (Guillaume 2011).

$$Qpcv = hcv.A\gamma.(Tr - Ta) \quad (16)$$

Aγ: Receiver Opening Surface

Tr: Receiver Temperature

Ta: Ambient Temperature

hcv: Convection Transfer Coefficient

The convection transfer coefficient is defined by (Guillaume 2011).

$$h_{cv} = \frac{N_u.\lambda}{d^2} \quad (17)$$

$$N_u = 0.664(R_e)^{1/2}(P_r)^{1/3} \quad (18)$$

$$R_e = \frac{V.d^2}{v} \quad (19)$$

V: Wind Speed

λ: Thermal Conductivity of Air

v: Air Viscosity

d: Receiver Diameter

3.2 Radiation Losses

These losses are influenced by the receiver's shape, but primarily by its temperature. They are directly related to the emissivity of the absorber (Guillaume 2011).

$$Q_{p.r} = \varepsilon . \sigma . A_{\gamma}(T_r{}^4 - T_{sk}{}^4) \quad (20)$$

ε: Emissivity Factor of the Absorber

σ: Stefan–Boltzmann Constant (5.670 × 10^-8 W/m^2.K^4)

Tsk: Sky Temperature

Typically, we consider the sky radiation temperature to be 6°C lower than the ambient temperature (Tsk = Ta – 6) [1].

3.3 Conduction Losses

These losses are associated with the characteristics of the equipment utilized, typically smaller in magnitude compared to convection or radiation losses. Often, they can be categorized alongside convection losses in most scenarios.

$$Q_{p.cd} = \lambda . A_{\gamma} . (T_r - T_a) \quad (21)$$

4. AUTOMATED TRACKING SYSTEM

Our prototype incorporates dual-axis tracking, both vertically and horizontally. We've meticulously engineered and manufactured parts and mechanisms to facilitate these movements. Automation is achieved through motors controlled by contactors (Arduino relay modules), which are in turn governed by an Arduino board. This Arduino board receives and processes signals from light sensors affixed to the reflector. Figure 5 provides a schematic overview of our implementation. Photoresistors generate analog values, which are then input to the Arduino board. Subsequently, the board executes a comparison using the programmed logic. It controls the operation of the Arduino relay modules, thereby activating the two motors to attain an optimal orientation toward the sun.

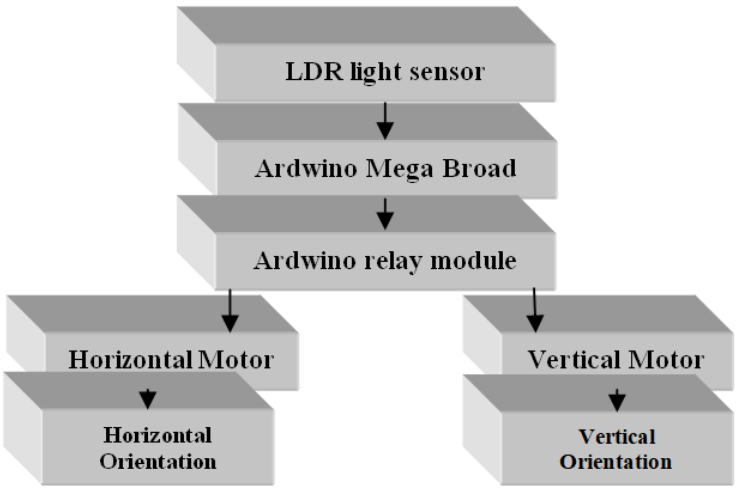

Fig. 5 Schematic Overview of Solar Tracking System

4.1 Arduino relay module

A relay module functions as a switch that can be controlled to establish a connection between the control section and the power section. It enables the opening or closing of a contactor within a power circuit based on a signal ranging from 0 to 5 volts. The relay comprises an electromagnet and a mechanical contactor. When the current surpasses a certain threshold at the input terminal, the electromagnet becomes magnetized, compelling the contactor to close the power circuit. Since there is no direct mechanical linkage between the control and power circuits (achieved through magnetic actuation), galvanic isolation exists between the two circuits. This isolation serves to safeguard the control circuit from potential harm.

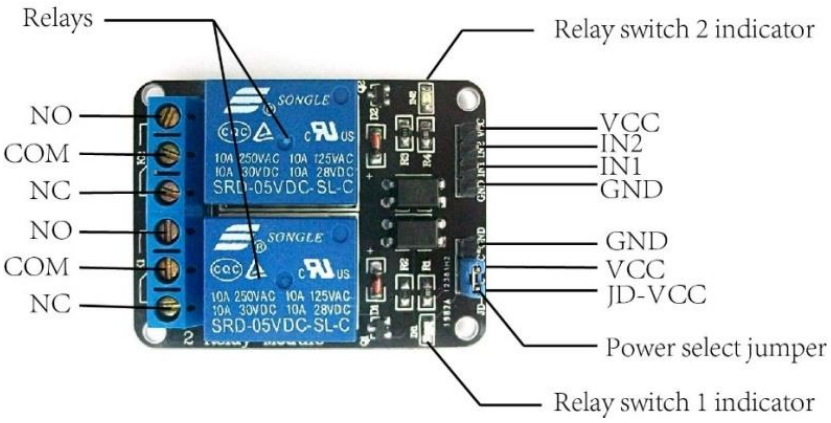

Fig. 6 Arduino relay module

4.2 Programming software

The Arduino module programming software is a versatile, cross-platform Java application that functions as both a code editor and compiler. It facilitates the transfer of firmware and programs via various serial links such as RS-232, Bluetooth, or USB, depending on the module (Guillaume 2011). The programming language employed is C++, compiled with avr-g++, and linked to the Arduino development library, enabling utilization of the board and its inputs/outputs. This standardized language implementation streamlines program development on Arduino platforms, particularly for individuals proficient in C or C++.

5. EVALUATION AND INTERPRETATION OF RESULTS

5.1 Execution of the experiment

Using thermocouples and a digital multimeter, we simultaneously measured five distinct temperatures: ambient temperature, the temperature inside the absorber, the temperature at the absorber's opening surface, and the temperature of the fluid at both the inlet and outlet of the absorber. Water served as the heat transfer fluid for conducting these tests, which were conducted at two separate locations, each under varying conditions.

5.2 First test

The experiment is scheduled to occur on 08/22/2022 in El Kseur, Algeria, commencing at 10:45 and concluding at 11:45. Measurements will be taken every 5 minutes, with a flow rate of 0.0016 liters per second. The weather conditions at the time of the experiment included clear skies and strong winds.

Geographical coordinates of El Kseur:

Latitude: 36°40′45″ North

Longitude: 4°51′19″ East

Altitude relative to sea level: 84 meters

The corresponding results are depicted in Table 3.

Figure 7 illustrates the temporal evolution of various temperatures. Notably, the ambient temperature and water inlet temperature exhibit minimal variation over time. Within 30 seconds of solar exposure, the temperature at the absorber's opening surface rises to 76°C, while the interior reaches 55°C, and the water outlet temperature registers at 39°C. Subsequently, over 30 minutes, these temperatures peak, reaching their maximum values: 125°C at the opening surface, 88°C internally, and 54°C at the water outlet. Following this peak, disturbances occur, particularly noticeable in the temperature at the absorber's opening surface.

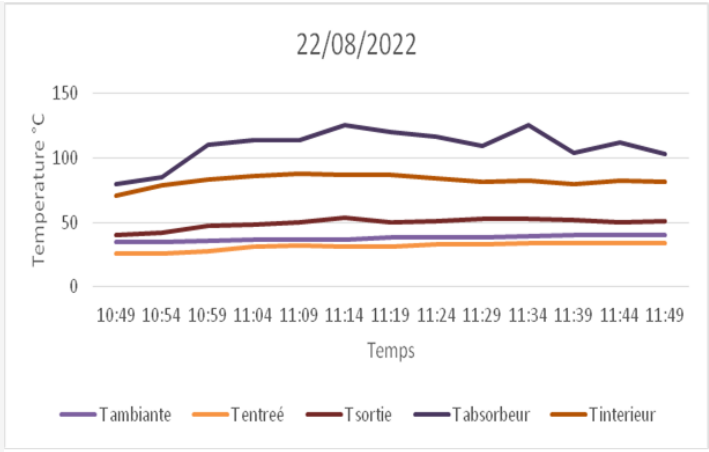

Fig. 7 Graph of temperature evolution as a function of time on 22/08/2022

Table 3 Measurement results from 22/08/2022

Hour	Ta	Te	Ts	Tab	Ti
10:49	32	28	39	76	55
10:54	35	26	40	80	71
10:59	35	26	42	85	79
11:04	36	28	47	110	83
11:09	37	31	48	114	86
11:14	37	32	50	114	88
11:19	37	31	54	125	87
11:24	38	31	50	120	87
11:29	38	33	51	116	84
11:34	38	33	53	109	81
11:39	39	34	53	125	82
11:44	40	34	52	104	80
11:49	40	34	50	112	82
11:54	40	34	51	103	81

We observed temperature fluctuations after 30 minutes into the experiment, attributable to the prevailing strong winds despite ample sunshine. These unfavorable conditions led to unsatisfactory results, prompting us to conduct another test.

5.3 Second test

The subsequent test was conducted on 09/08/2022 at the University of Bejaia, spanning from 12:00 p.m. to 2:05 p.m. Measurements were taken every 10 minutes, with a flow rate of 0.0022 liters per second. Weather conditions at the time included partly overcast skies and moderate wind.

Geographical coordinates of Bejaia:

Latitude: 39°54′26″ North

Longitude: 116°23′50″ East

Altitude relative to sea level: 49 meters

The corresponding results are depicted in Table 4.

Table 4 Measurement results from 08/09/2022

Hour	Ta	Te	Ts	Tab	Ti
12:05	30	32	38	102	43
12:15	32	26	38	100	70
12:25	33	32	47	124	80
12:35	30	29	50	116	84
12:45	31	30	50	113	85
12:55	31	32	52	110	83
13:05	32	36	56	113	86
13:15	33	34	62	126	85
13:25	33	34	63	116	86
13:35	34	34	68	121	99
13:45	34	36	57	105	84
13:55	34	36	62	127	81
14:05	35	36	61	122	87

The ambient temperature and water inlet temperature exhibit a nearly linear trend. After 30 seconds of solar exposure, the temperature at the opening surface reaches 102°C, while inside the absorber it reaches 43°C, and at the water outlet, it registers at 38°C. The peak temperatures achieved are as follows: 127°C at the opening surface; 99°C inside the absorber; 68°C at the water outlet.

Despite the partially overcast sky, the latest test yielded superior results. This suggests that the system is more affected by wind conditions than by diffuse radiation.

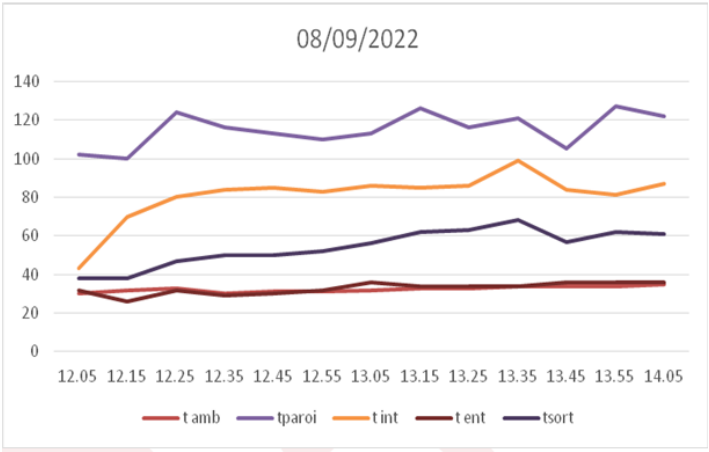

Fig. 8 Graph of temperature evolution as a function of time on 08/09/2022

5.4 Temperature at the absorber's surface and inlet in the absence of water flow

The temperature at the absorber's opening surface reached 382°C, exceeding that measured at the front, which reached 333°C. Inside the absorber, the temperature reached 241°C.

Fig. 9 Surface and Interior Temperatures of the Absorber

6. CONCLUSION

The objective of this project was to implement an automatic tracking system and develop an absorber to enhance the efficiency of the parabolic concentrator system. Key goals included replacing the actuator with an electric motor, designing a more efficient absorber, and creating a new program for improved stability and solar radiation monitoring. The results achieved were highly satisfactory: the automatic tracking system demonstrated enhanced stability and precision, while the absorber attained temperatures nearing 400°C. This temperature, four times higher than the boiling point of water at standard atmospheric pressure, signifies a significant energy source that could be harnessed for various applications. Consequently, the outlet temperatures of the heat transfer fluid were notably enhanced.

Through experiments conducted under diverse conditions and with varying parameters, it became evident that these systems are influenced by several factors, including solar illumination variations, reflector geometry, and choice of materials.

REFERENCES

A. Guillaume, «Modeling, dynamic simulation, experimental validation and energy optimization of a solar absorption cooling unit», Doctoral Thesis, University of Pau and Pays de l'Adour, November 28, 2011.

B.Stine. Michael Geyer, «Power from the sun», Lyle Centre for regenerative studies 2001.

D. Kedwards, L. Marlot. «Solar Sensors», Edition S CM Paris 1979.

GammaO.(2008). Study and production of a thermodynamic photovoltaic hybrid test bench. Master's dissertation, National College of Polytechnic, El-Harrach, Algeria.

Mohamed H. Ahmed. (2021) Performance of Solar Adsorption Cooling System with Different Solar Collectors Technologies. International Journal of Renewable Energy Research, Vol.11, No.2, June, 2021.

NadirN.(2012).Search for optimal operating conditions of a solar dryer. Master's dissertation, KasdiMerbah University, Ouargla, Algeria.

S. Bonned and A. Alaphilippe, «Thermodynamic conversion of solar energy in low or medium power installations». R. Energy 11th International Thermal Days. pp. 73-80. 2003.

Summary of the IEC 60584-1 standard on thermocouples, reference tables, and functions B

UH. Kurzweg and IP. Benson. «Iso-Intensity absorber Configurations For parabolic Concentrators», Solar energy Vol 29 No.2.pp167-174,1982.

Y. MEBARKI copy of course given for master students 2 electrical machines «Heating and cooling of electromechanical sharehold», at the University of Bejaia Algeria 2020.